

Original Research

Effect of Sweep Frequency Electromagnetic Field on CaCO_3 Scale Formation in Industrial Circulating Water

Bingcheng Liu, Xianpei Guo, Qiang Li*, Wenguang Jia, Hao Sun

Institute of Climate and Energy Sustainable Development, Qingdao University of Science and Technology,
No. 99 Songling Road, Qingdao 266061, China

Received: 21 March 2022

Accepted: 6 September 2022

Abstract

Electromagnetic field (EMF) treatment has demonstrated its superior efficiency and great potential in inhibiting scale formation in industrial plants. Despite the numerous studies focusing on improving the performance of EMF devices, there is still limited understanding of how the frequency affects the anti-scaling process. This problem restricts the development and optimization of the sweep frequency EMF technique, which is assumed to have a better anti-scale performance. In this work, experimental studies were performed to study the effect of the sweep frequency EMF on the precipitation of CaCO_3 under circulating flow conditions. The results showed that the sweep frequency EMF could stimulate the homogeneous crystallization of CaCO_3 in the simulated hard water solution, and the direct reaction between Ca^{2+} and HCO_3^- was the primary reaction route. The sweep frequency had a more pronounced effect on the scale formation process than the output current of the EMF device. The sweep frequency value was inversely correlated with the scale formation. The effect mechanism of sweep frequency on the scale formation process was discussed.

Keywords: sweep frequency, anti-scaling, correlation analysis, electromagnetic field, pH

Introduction

Scale deposits in water systems of industrial plants often lead to serious technical problems and economic losses through decreasing thermal transfer efficiency in heat exchangers and shortening the equipment life [1, 2]. Scales encountered in industrial applications include CaCO_3 , CaSO_4 , SrSO_4 , and BaSO_4 , amongst which CaCO_3 is the most common constituent [3-5].

Both chemical and physical treatment techniques were used in the past to inhibit scale formation. EMF is one of the typical physical anti-scaling methods that has attracted growing attention from lab researchers and field engineers due to its high efficiency and environmental protection.

Since the 1980s, over 4,000 studies about anti-scaling and anti-fouling with EMF have been reported [2, 6, 7]. EMF has proved its anti-scaling effectiveness through numerous applications and publications, indicating that EMF is an indispensable technique to control scale [8]. It was proposed that the EMF can accelerate the precipitation of mineral salts in bulk

*e-mail: qiangli@qust.edu.cn

solution and significantly reduce scale formation on pipes, heat exchangers and reverse osmosis (RO) membrane systems [9-12]. Efforts to further clarify the function mechanism of EMF are still ongoing for the enrichment of the associated scientific theory and the optimization of industrial applications.

Frequency is one of three essential properties of EMF that could affect the anti-scaling efficiency [6]. However, up to date, it has not been fully scientifically demonstrated how the frequency of EMF influences the anti-scaling process. Okazaki et al. [9] investigated the electromagnetic field treatment of hot spring water for scale inhibition and found that scale formation was inhibited when the frequencies of the applied electromagnetic field had value of 8 kHz, however, enhanced scale formation was found for frequencies of 4 and 6 kHz. Carnahan et al. [13] studied the effects of EMF frequency on salt and water transport in commercial and lab-scale RO membranes. Probably due to the frequency being too low, during more than 500 hours of operation, they observed no difference in salt permeability when the frequency of EMF was varied from 40 to 300 Hz. Tijing et al. [14] found that the efficiency of EMF in the precipitation of fouling increased with the increase of frequency. They suggested that ions had more probability of colliding at a higher frequency; thus, the scale precipitation rate in the bulk water was accelerated. Wang et al. [15] investigated the vibration of solubility of calcium carbonate with an EMF frequency of 1 kHz, 10.3 kHz, and 15.4 kHz; the best result was observed when the frequency was 1 kHz. They explained that hydrogen bond has an increased probability of being broken apart when the frequency of EMF is the same as that of the natural frequency of water. Chen et al. [16] noticed that the formation process of scales was different for different frequencies. So they suggested that CaCO_3 scale formation could either be enhanced or prohibited, or the scale structure being changed, depending on the specific frequency value.

Compared with the fixed frequency EMF treatment, a sweep frequency EMF treatment was suggested to have a better anti-scaling performance [16-18]. Xia also held the same idea and pointed out that circulating water magnetization losses occurred under the fixed frequency pulsed square wave magnetic field. The higher the frequency, the higher magnetization loss was [19]. Chen et al. [20] investigated the anti-fouling performance on the heat exchanger surface under sweep frequency of EMF at 1-13 kHz and 13-25 kHz. They found that the calcite mass fraction in the scale sample decreased from 100% to 65.31%, and the mass fraction of aragonite increased to 34.69%. The scale became loose and could be washed away more easily at 13-25 kHz. The relationship between the anti-scaling performance and different sweep frequencies was not investigated. To elucidate the underlying mechanism of sweep frequency affecting the scale formation processes remains the problem to be solved.

Based on our previous studies of optimizing the output parameters of an EMF device [21, 22], this work aimed to further explore the effect of sweep frequency EMF on the CaCO_3 scale formation. An extended range of sweep frequency EMF treatment was applied to the simulated industrial hard water solution, which flowed through the test section by a circulating device. The variation of solution pH, conductivity, particle diameter distribution, scale thickness, and the mass increase of the coupon was measured. The effect mechanism of sweep frequency on the scale formation process was discussed.

Material and Methods

Experimental Setup

The setup used in experiments is shown in Fig. 1 [22]. The system was composed of an EMF control unit, a PVC pipe (the radius was 100 mm), and 100-turn tightly wound coils. The coils were made up of a polyvinyl chloride insulated flexible cable with a copper core, which had a conductor diameter of 5.3 mm and an insulation layer thickness of 0.8 mm.

For the experimental group, the output sweep frequency of the EMF control unit was set to 65~70 kHz, 70~75 kHz, 75~80 kHz, and 80~85 kHz, respectively. The output voltage was 60 V, and the output waveform was a square wave. Fig. 2 shows an example of how the EMF control unit works. The output frequency continually increased from the low frequency (F_d) to the high frequency (F_u), the number of periods of each frequency (n) was one, and the frequency step gain (h) was 500. When the high frequency was reached, it returned to the low frequency and started a new cycle. The experiment without the EMF treatment was used as the control group.

In this study, a Seven Excellence™ tester (Mettler Toledo) was used to measure the solution pH and conductivity. The test range of the conductivity tester was 0.1-9999 $\mu\text{S}/\text{cm}$, and the measurement accuracy was $\pm 5\%$. The measuring range of the pH tester was -2 to 20, and the limit of measurement error was ± 0.002 . Meanwhile, the particle diameter in the solution was detected by a laser particle size analyzer (Winner 2003A, Winner Particle Instrument Company), and its detection range was 0.1-2000 μm . The laser profile sensor used to measure scale thickness in this experiment was LP-S5050, and the data processing software was LP-GUIDE2. The weight of coupons was weighted by an electronic balance (JA2003), which has an accuracy of 1 mg.

Material and Testing Methods

As the most common constituent of scales in industrial circulating water systems, CaCO_3 was added to tap water to simulate the hard water solution. In this

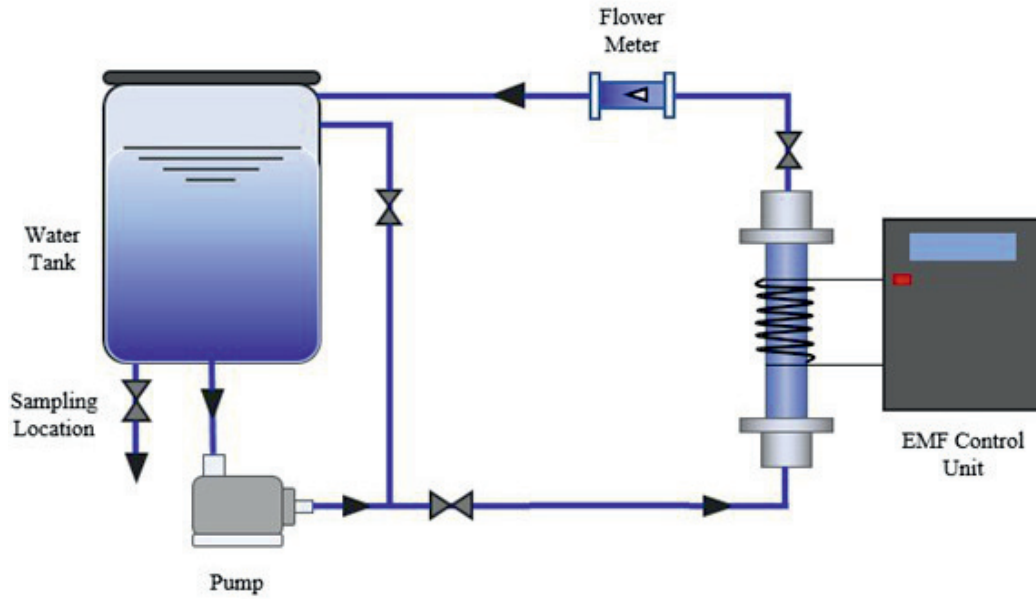


Fig. 1. A schematic diagram of the circulating flow test device.

study, 111 g CaCl_2 and 168 g NaHCO_3 were added to 100 L tap water so that the hardness of the solution was 1000 ppm of CaCO_3 . The temperature of the solution was maintained at $25 \pm 2^\circ\text{C}$. As shown in Fig. 1, the hard water solution was transported from the water tank to the test section by a pump and then flowed back to the water tank. The flow velocity was 0.6 m/s.

In the test section, a coupon was installed close to the solenoid coil to study the CaCO_3 scale formation rate on the steel surface under the treatment of EMF. The material of the coupon was stainless steel (18% Cr, 9% Ni and 70% Fe) with a dimension was 38 mm×15 mm 2 mm. The surface of the coupon was ground from smooth to rough with an abrasive paper (120 Cw), aiming to accelerate the scaling process [23]. Due to the heating effect of EMF on high magnetic permeability materials, the stainless steel coupon could have an increase in the temperature. To reduce this effect, putting the stainless coupon in a position away from the solenoid coil, or using coupons made of copper or plastic materials are suggested.

As soon as the experiment began, 200 ml of test solution sample was collected every 10 minutes for pH and conductivity measurement in the first hour. Then, the same process was repeated every 30 minutes for the next 3 hours. After the experiment, particle diameter in the solution was measured by the laser particle size analyzer. The coupons were removed from the test section and dried in a drying oven. The distance between the laser source and test bench was set to 40 mm, and the coupons were put on the test bench to observe the distance of specimens to the laser source. Then, the coupons were weighted by the electronic balance. The weight of the coupon was recorded as G_1 (the initial weight of the coupon was recorded as G_0). The scale formation rate was calculated through Eqn. 1 as follows:

$$D = \frac{(G_1 - G_0)}{G_0} \times 100\% \quad (1)$$

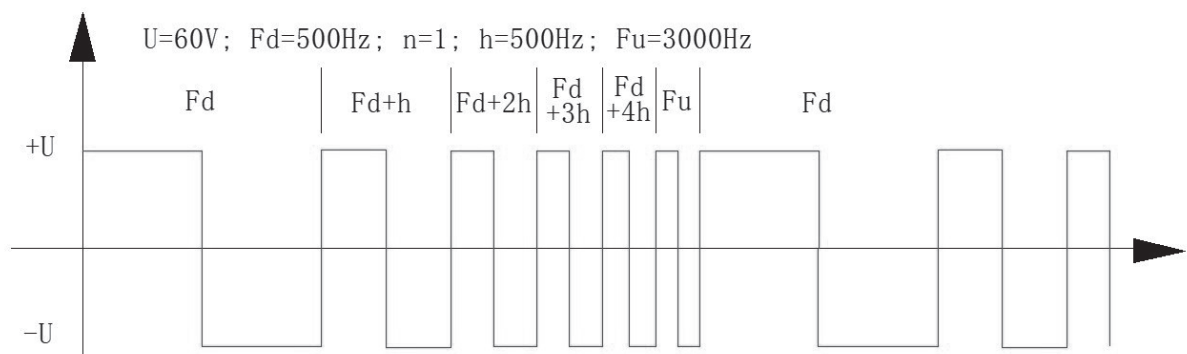


Fig. 2. An example showing the working logic of the output sweep frequency.

Results and Discussion

Variation of Current in the Solenoid Coil

The current in the solenoid coil was recorded, and the average current was determined by averaging the maximum and minimum current for the sweep frequency range. The average current under different sweep frequencies is shown in Fig. 3. It shows that the average current decreases when the sweep frequency is increased. This is because induction resistance in the solenoid coil increased with the increasing frequency. When a constant voltage is applied, the current thus decreases.

Variation of Solution pH Value

The solution pH after EMF treatment with different sweep frequencies is shown in Fig. 4. For all the testing conditions, with or without EMF treatment, solution pH decreased as the testing time was increased. For the first 60 minutes, the pH values of the hard water solution in all experiments decreased significantly. After that, the pH value continued to drop but at a relatively lower rate and became stable after 240 minutes.

The decrease of solution pH is attributable to the formation of CaCO_3 , as shown in Eqn. 2, which includes the following reactions (Eqn. 3-6) [24]:

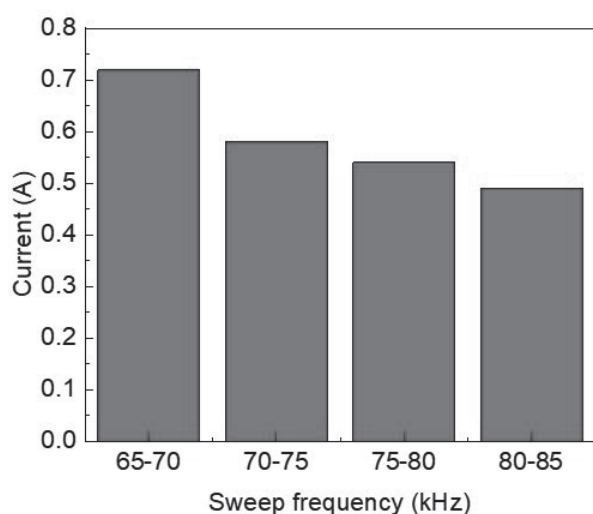
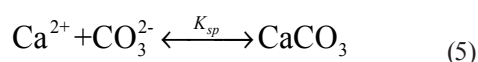
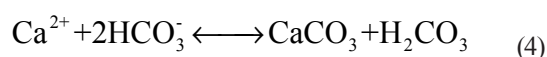
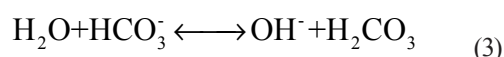


Fig. 3. Average current in the solenoid coil under different sweep frequency.



The solution was alkaline ($\text{pH} = 7.8$) at first due to the high concentration of bicarbonate ions. Fig. 5 shows the fraction of carbonate acid, bicarbonate, and carbonate in the solution as a function of pH at 25°C [25]. At the pH range of 7.1~7.8, HCO_3^- is the dominant ion in the solution, followed by $\text{CO}_2/\text{H}_2\text{CO}_3$ and CO_3^{2-} , which is ranked by the concentration value of these species. The negligible concentration of CO_3^{2-} ion determines that the Eqn. 4 could be the primary route for forming the CaCO_3 scale.

At the beginning of the experiment, CaCO_3 scale forms quickly due to the high concentration of Ca^{2+} and HCO_3^- . The scale continues to form until the formation rate of CaCO_3 equals its dissolution rate. During this process, both the concentration of Ca^{2+} and HCO_3^- gradually decreases, the formation rate of CaCO_3 scale also decreases. Therefore, the solution pH drop rate becomes more and more slowly.

The pH drop in the control group was smaller than that with the EMF treatment, showing that the formation rate of CaCO_3 scale in the hard water solution with EMF treatment is higher than that of the control group. And the pH drop varied after the EMF treatment with different sweep frequencies, i.e., a higher pH drop was associated with a lower sweep frequency. Obviously, the sweep frequency of EMF does affect the scale formation process, as the results observed elsewhere in the literature [14-16], the possible mechanism is discussed in a later section of this work.

Variation of Solution Conductivity

Variation of solution conductivity of hard water solution after the EMF treatment with different sweep

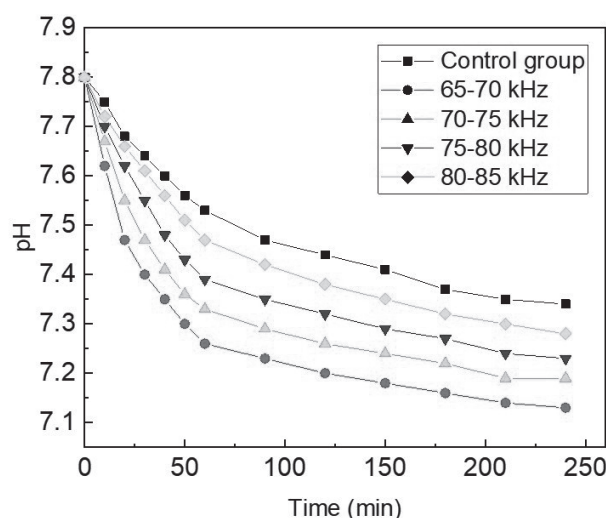


Fig. 4. Variation of solution pH with EMF treatment of different sweep frequencies.

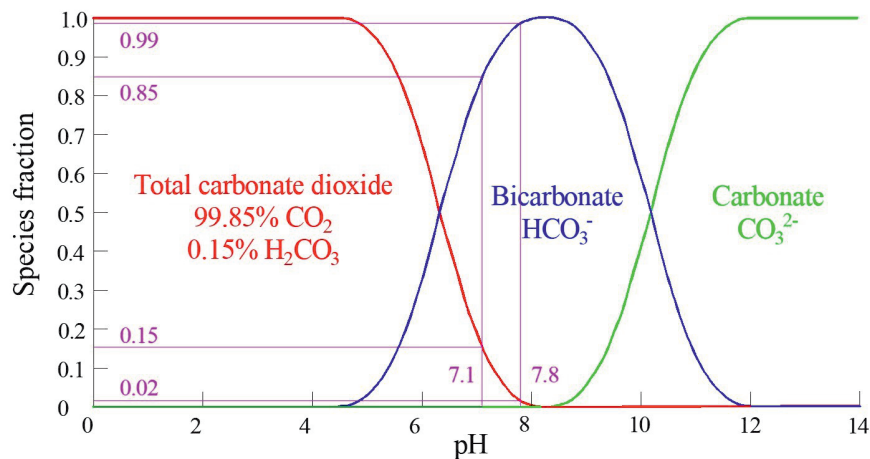


Fig. 5. Fraction of species in the carbonized solution as a function of solution pH at 25°C (Reproduced with permission from [25], © MDPI 2021).

frequencies is shown in Fig. 6. It can be found that the variation of solution conductivity as a function of EMF sweep frequency follows the same trend as that of the solution pH. For all the test conditions, solution conductivity decreased as test time was prolonged. The decrease rate was relatively fast for the first 60 minutes and then became more and more slowly. Compared with the control group, the solution conductivity values of the hard water solution with EMF treatment were lower. The solution conductivity values were also different when the sweep frequency was varied. A lower conductivity was associated with a lower sweep frequency.

Solution conductivity is proportional to the total concentration of all charged ions in the solution. So a high solution conductivity means a high concentration of charged ions in the solution. The formation process of the CaCO_3 scale, as indicated in Eqn. 4, is a charged ion

neutralization process. Therefore, solution conductivity gradually decreased as the formation of CaCO_3 process proceeded, and the decrease rate was affected by the decrease of the formation rate. The variation of solution conductivity is thus another evidence of the effectiveness of EMF on scale formation.

Variation of Particle Diameter

As shown in Fig. 7, the diameter of particles in the hard water solution was between 0.7 and 50 μm . The curves of particle diameter distribution after the EMF treatment are all at the right of the curve of the control group. This result indicates that particle diameters were larger after the treatment with EMF. And as the sweep frequency decreased, these curves gradually moved to the right, which means the particle size grew bigger. Besides, the curve peak dropped

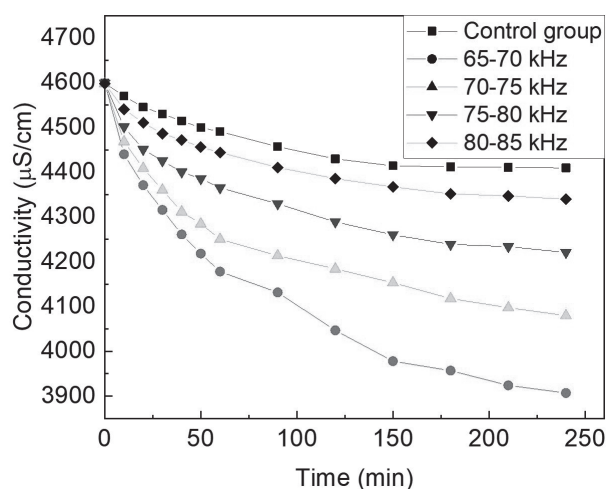


Fig. 6. Variation of solution conductivity with EMF treatment of different sweep frequencies.

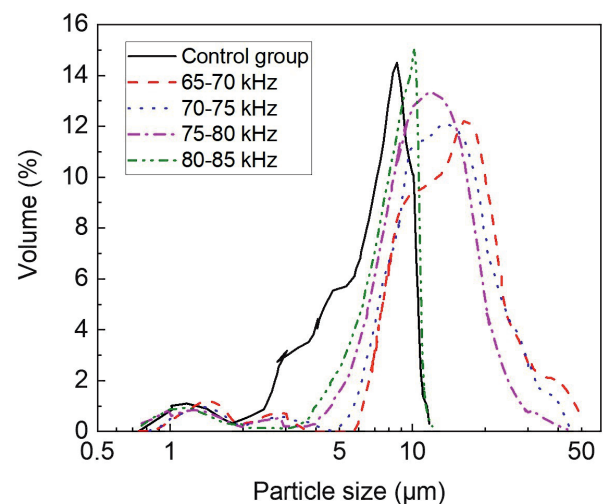


Fig. 7. The particle size distribution of the dynamic experiment.

Table 1. Parameters of particles in the solution and scale formation after treatment for 240 min.

	Control group	65~70 kHz	70~75 kHz	75~80 kHz	80~85 kHz
Average particle diameter (μm)	8.35	15.24	13.96	12.16	10.88
Scale thickness, d (mm)	0.85	3.64	2.76	2.12	1.72
Scale formation rate, D (%)	2%	73%	58%	41%	31%

slowly in general when sweep frequency was smaller, indicating that the difference in the diameter of particles gradually became smaller.

The average particle diameter in the hard water solution after the EMF treatment for 240 minutes was calculated and summarized in Table 1. It illustrates that the average particle diameter increased with the decrease of sweep frequency. Similar results were also observed by other researchers [26, 27]. Donaldson et al. [26] attributed this phenomenon to the effect of electromagnetic fields on the nucleation process. Yang et al. [27] proposed that electromagnetic field increased the nucleation rate, and increased the diameter by 10% ~30%.

Generally, nucleation and growth are the two processes of scale formation [28], in which supersaturation (SS) is a precondition [2]. SS can be calculated by $[\text{Ca}^{2+}][\text{CO}_3^{2-}]/K_{sp}$ (K_{sp} is the solubility of CaCO_3). To meet the condition of promoting the growth process, SS should always be greater than 1, then a large $[\text{Ca}^{2+}][\text{CO}_3^{2-}]$ or a smaller K_{sp} is expected. $[\text{Ca}^{2+}]$ and $[\text{CO}_3^{2-}]$ become smaller as precipitation proceeds, especially when $[\text{Ca}^{2+}]$ and $[\text{CO}_3^{2-}]$ are not replenished in the solution, which is the case in this work. So K_{sp} is supposed to decrease after the treatment of EMF.

Variation of Weight and Thickness of the Scales on the Coupons

The thickness and weight of the scale formed on the steel coupons were measured after exposure to the hard water solution. The thickness of scales on the steel coupons cannot be measured directly. Instead, it was calculated by subtracting the distance between the laser source and the initial coupon from the distance between the laser source and the coupon with scales. The distance between the laser source and all coupons under all sweep frequencies is shown in Fig. 8, which shows that the distance from the surface of the coupons to the laser source gradually became smaller. This result means scales formed on the steel coupon surface. The distance is smaller for coupons after EMF treatment, compared with that of the control group. In addition, the distance for coupons under lower sweep frequency EMF treatment is smaller than that with high sweep frequencies. So more scales were formed on the steel coupon surface after EMF treatment, especially under lower sweep frequencies. The average thickness of scales on the steel coupons was calculated and was summarized in Table 1. The weight of the steel coupons

after exposure in the hard water solution was measured, with which the scale formation rate was calculated and summarized in Table 1. It shows that the scale formation rate is higher after being treated with EMF than the control group. Scale formation rate was different for different sweep frequencies, and a relatively higher scale formation rate was seen for a smaller sweep frequency. Basically, this result was consistent with the trend of the scale thickness.

There are two crystallization pathways for scale formation, surface crystallization and bulk crystallization [6]. The former is also called heterogeneous crystallization that happens on the surface, while the latter is called homogeneous crystallization, which mainly happens in the solution. According to the enhanced pH drop, conductivity drop, and larger particle diameter, it can be concluded that homogeneous crystallization was promoted in the presence of the sweep frequency EMF. Although more scales formed on the coupon surface after the EMF treatment, it doesn't mean the EMF treatment promotes heterogeneous crystallization. When a coupon is put in the test section, the electromagnetic field generated from the solenoid coil will affect the water molecules and ions in the solution and the stainless steel coupon. For the steel coupon, the solenoid coil with high sweep frequency acts as a heater, which is similar to the working mechanism of an induction cooktop. An increase in temperature could cause a faster rate of

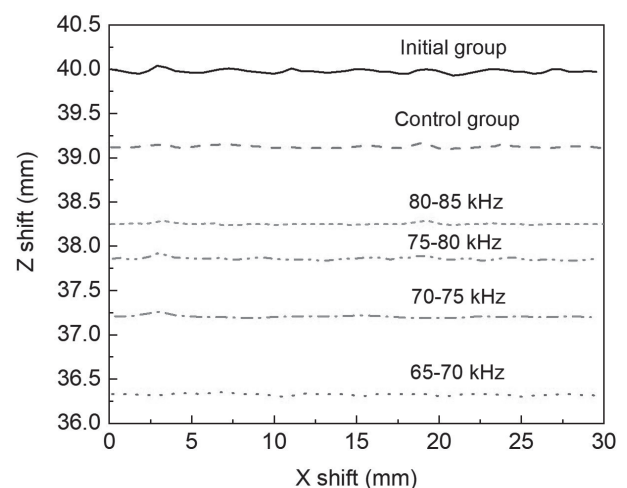


Fig. 8. The distance between the laser source and coupons after EMF treatment with different sweep frequencies.

Table 2. Pearson's correlation coefficients between various factors.

	Sweep frequency	Average current
Average current	-0.954	--
pH drop	-0.986	0.965
Conductivity drop	-0.994	0.980
Average particle diameter	-0.998	0.942
Scale thickness	-0.986	0.984
Weight change rate	-0.995	0.961

surface scaling. CaCO_3 scale will thus preferentially form on the hot surface. As a result, more scales were formed on the coupons treated by the sweep frequency EMF than the control group.

Effect of Sweep Frequency EMF Treatment on the Scaling Process

A correlation analysis was made based on the above-mentioned experimental results (as summarized in the Appendix). The Pearson's correlation coefficients between sweep frequency and various factors, including average current, pH drop, conductivity drop, average particle diameter, scale thickness, and weight change rate, were determined using the Data Analysis tool embedded in Microsoft Excel software [29] and are shown in Table 2. Considering that the average current is also an important factor for the water treatment, as it is proportional to the energy output of the EMF device and the induction magnetic field intensity in the hard water solution, the Pearson's correlation coefficients between the average current and those factors were also determined.

As mentioned above, the average current decreased with the increasing sweep frequency. Accordingly, the correlation coefficient between the sweep frequency and the average current was negative, i.e., -0.954, indicating an inverse correlation. Since this value is very close to -1, the correlation between the sweep frequency and the average current is significant.

From Table 2, it can be found that the sweep frequency always has a more significant correlation coefficient with the pH drop, conductivity drop, and so on, than that of the average current, indicating a more pronounced effect of sweep frequency on the scale formation process. This result once again proved the significant role of frequency as one of the three essential properties of EMF in anti-scaling applications.

Despite the inconsistent results of the anti-scaling performance of EMF treatment in the literature, the EMF was commonly believed to affect the scale formation process by two distinct mechanisms: hydration effects and magnetohydrodynamic

phenomena [30]. For the hydration effect, the magnetic field exerted on the solution alters the hydrating structure of water molecules in the vicinity of the ions, including changing the orientation of proton spin and breaking large water molecule groups into small ones, thus promoting mobility of Ca^{2+} and HCO_3^- ions. Magnetohydrodynamic phenomena are based on the Lorentz forces that exit when the fluid flows and the EMF is present. The motion of charged species in the solution can be affected by the Lorentz force when they pass through the EMF as [31]:

$$|F_L| = q|v \times B| = qvB\sin\theta \quad (7)$$

where F_L is the magnitude of the Lorentz forces, q is the number of charge, v is the flow velocity, B is the magnetic field strength, and θ is the angle between v and B vectors.

When a time-varying magnetic field is produced in the cavity of a solenoid coil due to the alternating electric current, an electric field is induced simultaneously, according to Faraday's law:

$$\int_c E \cdot dl = - \int \frac{\partial B}{\partial t} \cdot dS \quad (8)$$

where E is the induced electric field intensity vector, l is the circumferential vector, c is an arbitrary closed path, and S is the curved surface vector with the border of c .

The combined effects from the EMF treatment stimulate all charged species in the test solution, including calcium ions and bicarbonate ions, causing a faster collision frequency. Therefore, the probability and efficiency of CaCO_3 precipitation are enhanced, with an increase in both the precipitate size and quantity. A larger decrease of solution pH and conductivity after EMF treatment was thus observed in the presence of EMF.

Since the magnetic intensity is proportional to the current, thus it is negatively correlated with the frequency of EMF when the output voltage remains unchanged. The inductive magnetic intensity decreases when the sweep frequency increases, which means both the hydration effect and the magnetohydrodynamic phenomena decrease. Although there is a high variation rate of the magnetic field at a high sweep frequency, the reduced electric field intensity also decreases due to the decreasing magnetic intensity. As a result, the precipitation rate and crystal size under high sweep frequency are lower than that of low sweep frequencies.

It seems that when the output voltage keeps constant, a lower sweep frequency is better for the EMF treatment of the hard water solution. However, this is not always true as the effect of EMF is very complex. For example, it was suggested that when the sweep frequency equals the frequency of water molecules, the water molecule groups are more easily to break due to the resonance effect. Thus ions are more easily to be released from

the water molecule group. Because the frequency of natural water molecules is affected by many factors, including temperature, pH, hardness, etc., it is difficult, if not possible, to determine the exact frequency value. If the sweep frequency happens to equal this value, the precipitation is sure to be enhanced. However, the effect of sweep frequency is still open to further study to illustrate the exact mechanism, which is the motivation for our ongoing studies.

Conclusions

In this work, experimental studies were performed to study the effect of the sweep frequency EMF

treatment on the formation of CaCO_3 under circulating flow conditions. The results showed that the sweep frequency EMF could stimulate the homogeneous crystallization of CaCO_3 in the simulated hard water solution, in which the direct reaction between Ca^{2+} and HCO_3^- was the primary reaction route. The sweep frequency has a more pronounced effect on the scale formation process than the output current of the EMF device. The sweep frequency EMF treatment increased the mobility of Ca^{2+} and HCO_3^- ions and introduced various forces, thus causing a high collision rate, which is beneficial for the CaCO_3 scale formation. Although the sweep frequency was inversely correlated with the scale formation, it doesn't mean a lower sweep frequency is a better choice.

Appendix

Table A1. Summation of the experimental results.

Group	Frequency*	Average current	pH drop**	Conductivity drop***	Average particle diameter	Scale thickness	Weight change rate
	Hz	A		$\mu\text{S}/\text{cm}$	μm	mm	%
65~70 kHz	67500	0.72	0.78	662	15.24	3.64	73%
70~75 kHz	72500	0.58	0.7	478	13.96	2.76	58%
75~80 kHz	77500	0.54	0.67	342	12.16	2.12	41%
80~85 kHz	82500	0.49	0.59	230	10.88	1.72	31%

* Frequency in the table was arbitrarily determined by averaging the maximum and minimum frequency value of a frequency range, and this value was verified to have a negligible effect on the determined correlation coefficient.

**The pH drop for each group was determined by subtracting the solution pH after 4-hour experiment from the initial solution pH.

***Conductivity was determined by subtracting the conductivity after 4-hour experiment from the initial conductivity.

Acknowledgments

This work was supported by the Key Technologies Research and Development Program of China (No. 2017YFB0603300), the Shandong Province Natural Science Foundation (No. ZR2019BEE040), and the Department of Science & Technology of Shandong Province (No. ZR2018LB025).

Conflict of Interest

The authors declare no conflict of interest.

References

- LI J., TANG M., YE Z., CHEN L., ZHOU Y. Scale formation and control in oil and gas fields: A review. *J. Dispersion Sci. Technol.* **38** (5), 661, **2016**.
- ALABI A., CHIESA M., GARLISI C., PALMISANO G. Advances in anti-scale magnetic water treatment. *Environ. Sci.: Water Res. Technol.* **1** (4), 408, **2015**.
- XU X., LIN L., PAPELIS C., MYINT M., CATH T.Y., XU P. Use of drinking water treatment solids for arsenate removal from desalination concentrate. *J. Colloid Interface Sci.* **445**, 252, **2015**.
- LIN L., XU X., PAPELIS C., CATH T.Y., XU P. Sorption of metals and metalloids from reverse osmosis concentrate on drinking water treatment solids. *Sep. Purif. Technol.* **134**, 37, **2014**.
- LIN L., XU X., PAPELIS C., XU P. Innovative use of drinking water treatment solids for heavy metals removal from desalination concentrate: Synergistic effect of salts and natural organic matter. *Chem. Eng. Res. Des.* **120**, 231, **2017**.
- LIN L., JIANG W., XU X., XU P. A critical review of the application of electromagnetic fields for scaling control in water systems: mechanisms, characterization, and operation. *npj Clean Water.* **3** (1), 1, **2020**.
- GARCÍA S., TRUEBA A. Influence of the Reynolds number on the thermal effectiveness of tubular heat exchanger subjected to electromagnetic field-based antifouling treatment in an open once-through seawater cooling system. *Appl. Therm. Eng.* **140**, 531, **2018**.
- PIYADASA C., RIDGWAY H.F., YEAGER T.R., STEWART M.B., PELEKANI C., GRAY S.R., ORBELL J.D. The application of electromagnetic fields to the

- control of the scaling and biofouling of reverse osmosis membranes - A review. *Desal.* **418**, 19, **2017**.
9. OKAZAKI T., UMEKI S., ORII T., IKEYA R., SAKAGUCHI A., YAMAMOTO T., WATANABE T., UEDA A., KURAMITZ H. Investigation of the effects of electromagnetic field treatment of hot spring water for scale inhibition using a fibre optic sensor. *Sci. Rep.* **9** (1), 10719, **2019**.
 10. PIYADASA C., YEAGER T.R., GRAY S.R., STEWART M.B., RIDGWAY H.F., PELEKANI C., ORBELL J.D. The influence of electromagnetic fields from two commercially available water-treatment devices on calcium carbonate precipitation. *Environ. Sci.: Water Res. Technol.* **3** (3), 566, **2017**.
 11. ROUINA M., KARIMINIA H.-R., MOUSAVI S.A., SHAHRYARI E. Effect of electromagnetic field on membrane fouling in reverse osmosis process. *Desal.* **395**, 41, **2016**.
 12. JIANG W., XU X., LIN L., WANG H., SHAW R., LUCERO D., XU P. A Pilot Study of an Electromagnetic Field for Control of Reverse Osmosis Membrane Fouling and Scaling During Brackish Groundwater Desalination. *Water.* **11** (5), **2019**.
 13. CARNAHAN R.P., BARGER M., GHIU S. Impact of magnetic fields on reverse osmosis separation: A laboratory study. Report, University of South Florida, **2005**.
 14. TIJING L.D., KIM H.Y., LEE D.H., KIM C.S., CHO Y.I. Physical water treatment using RF electric fields for the mitigation of CaCO_3 fouling in cooling water. *International J. Heat and Mass Transfer.* **53** (7), 1426, **2010**.
 15. WANG J.G., FENG Y., ZHANG X.M., LIU X.M. Effects of alternating electromagnetic field on calcium carbonate scaling process. 2011 International Conference on Informatics, Cybernetics, and Computer Engineering (ICCE2011), Melbourne, Australia, **2011**.
 16. CHEN J., XIONG L., HU G., YANG Z., MIAO X., WU Y. Experimental research on the frequency effects of high-frequency electromagnetic pulse on the treatment of industrial circulating water. *Ind. Water Treat.* **34** (12), 71, **2014** [In Chinese].
 17. LUO Q.M., WANG J.X., YAN C.J., ZHANG J.B., WANG Z.Y., PAN H., ZHANG B., ZHONG Y., LI D., ZHANG Z.H. Research And Application of Frequency Conversion Electromagnetic Anti-scale. *Drill Prod. Technol.* **43** (3), 4, **2020** [In Chinese].
 18. WANG J.G., LIANG Y.D., YIN Z., WANG Y.R. A Research Review of Electromagnetic Anti-scale Effect and its Mechanism. *J. Northeast Dianli University.* **36** (6), 6, **2016** [In Chinese].
 19. XIA T. Study on crystallization kinetics and crystallization behavior of CaCO_3 of circulating water under the electromagnetic field. Master's thesis, Inner Mongol University of Technology, Hohhot, China, **2015** [In Chinese].
 20. CHEN X., ZHAO J., ZHANG B., ZHANG A. Effect of electromagnetic field on scaling process on heat exchange surface. *J. Eng. Therm. Energ. Power.* **35** (2), 155, **2020** [In Chinese].
 21. LIU B., SUN H., LIU N., LI C., ZHANG M., JIA W. Experimental study on the influence of sweep frequency electromagnetic anti-fouling technology on industrial circulating water. *J. Water Supply: Res. Technol.-Aqua.* **68** (1), 1, **2019**.
 22. LIU B., LIU N., WANG S., JIA W. Effect of output parameters of electromagnetic anti-fouling technology. *International J. Appl. Electromagn. Mech.* **62**, 433, **2020**.
 23. ALIM F., TLILI M.M., AMOR M.B., MAURIN G., GABRIELLI C. Effect of magnetic water treatment on calcium carbonate precipitation: Influence of the pipe material. *Chem. Eng. Process.* **48** (8), 1327, **2009**.
 24. HAN Y., ZHANG C., ZHU L., GAO Q., WU L., ZHANG Q., ZHAO R. Effect of alternating electromagnetic field and ultrasonic on CaCO_3 scale inhibitive performance of EDTMPS. *J. Taiwan Inst. Chem. Eng.* **99**, 104, **2019**.
 25. MARTÍNEZ MOYA S., BOLUDA BOTELLA N. Review of Techniques to Reduce and Prevent Carbonate Scale. *Prospecting in Water Treatment by Magnetism and Electromagnetism. Water.* **13** (17), **2021**.
 26. DONALDSON J., GRIMES S., editors. Control of scale in sea water applications by magnetic treatment of fluids. SPE Offshore Europe, Aberdeen, United Kingdom, **1987**.
 27. YANG J., YANG Z., SHI J., JIANG S. The effect of magnetic field on the crystalline dynamics with a new type of carbonating column. *J. Beijing University Chem. Technol.* **24** (2), 1, **1997** [In Chinese].
 28. ALOMARI A.A. Effect of Magnetic Treatment on Temporary Hardness of Groundwater. *Asian Journal of Chemistry.* **31** (5), 1017, **2019**.
 29. CARLBERG C. Regression analysis microsoft excel. Que Publishing, **2016**.
 30. KNEZ S., POHAR C. The magnetic field influence on the polymorph composition of CaCO_3 precipitated from carbonized aqueous solutions. *J Colloid Interface Sci.* **281** (2), 377, **2005**.
 31. SILVA I.B., QUEIROZ NETO J.C., PETRI D.F.S. The effect of magnetic field on ion hydration and sulfate scale formation. *Colloids Surf. A.* **465**, 175, **2015**.

